FUDMA Journal of Sciences (FJS)
ISSN online: 2616-1370
ISSN print: 2645 - 2944
Vol. 6 No. 3, June, 2022, pp 271 - 277
DOI: https://doi.org/10.33003/fjs-2022-0603-999

PAIR INTERACTION OF ACTIVE COLLOIDS IN AN EXTERNAL CHEMICAL GRADIENT

***Yahaya Ibrahim and Saratu Abdulfatah**

Department of Physics, Umaru Musa Yar'adua University, P.M.B. 2218 Katsina, Nigeria

*Corresponding authors' email: **yisarki@gmail.com;**

ABSTRACT

We study the pair interaction of chemically isotropic active colloidal particles in an externally imposed chemical gradient. Colloid particles migrate in response to a gradient of chemical solutes (i.e., via the diffusiophoresis mechanism). The particles motion induces fluid flow and distort locally the background chemical concentration field. Using the methods of images, we calculate the phoretic inter-particle interaction between two symmetric active colloids in the presence of an externally applied gradient. We highlight an interesting colloidal dipole that would arise from tuning the surface and chemical activity of the colloids. The colloidal phoretic dipoles share similar properties to the electrostatic dipoles. The inter-particle interaction we obtained is an important component for a large-scale simulation of the active colloid suspension. It may also help towards better understanding of the active systems' emergent phenomena.

Keywords: active soft matter, colloids, diffusiophoresis, non-equilibrium dynamics, stokes flow

INTRODUCTION

Active (or "Living") matter systems have attracted the attention of the scientific community in recent years (S. J. Ebbens & Howse, 2010; Golestanian et al., 2007; Howse et al., 2007; Kreuter et al., 2013; Moran & Posner, 2017; Palacci et al., 2013; Paxton et al., 2005). These active matter systems are usually far from equilibrium and they consume energy at the level of individual particles rather than driven by energy supplied through a boundary. Active matter systems are composed of mesoscopic active particles which self-propel (or self-rotate) at the individual particle level. Natural examples include flock of fish, microscopic living organisms such bacteria and other motile single cell organisms. One of the widely studied artificial active particles is the half-coated platinum polystyrene beads that self-propels in a hydrogen peroxide solution (S. Ebbens et al., 2014; Howse et al., 2007; Kreuter et al., 2013; Moran et al., 2010; Paxton et al., 2005). These systems, both natural and artificial, exhibit interesting emergent phenomena such as dynamic cluster formation (Buttinoni et al., 2013; Navarro & Fielding, 2015; Theurkauff et al., 2012) and motility-induced phase separation (Cates & Tailleur, 2015) among others (Eze & Joseph, 2018).

Experimentally, (Theurkauff et al., 2012) explored the behaviour of a two-dimensional dense suspension of artificially fabricated active colloids. (Theurkauff et al., 2012) half-coated micron sized gold bead with platinum. The authors observed emergence of a novel dynamic cluster phase, with fluctuating cluster size when the colloids were suspended in a hydrogen peroxide (H_2O_2) solution. The authors attribute the observed phenomenon to diffusiophoretic interaction between the active colloids. An interested reader can find a comprehensive review on both experiments and theory of such systems by (Bialké et al., 2015).

(Soto & Golestanian, 2014) performed extensive molecular dynamics simulation of isotropic active colloid particles. The authors predicted dynamic self-assembling "molecules" that could exhibit novel interaction pattern which breaks the action-reaction symmetry we are familiar with from equilibrium dynamics. Recent theoretical work in this direction continue to further our understanding of these novel active materials (Jewell et al., 2016; Negro et al., 2022; Wagner et al., 2021).

Most of the experimentally studied active colloid systems are powered by a chemical reaction. Thus, it's expected that self-diffusiophoresis could be the dominant propulsion mechanism for these systems. Self-diffusiophoresis is the migration of a chemically active colloid due to self-generated chemical concentration gradient (J. Anderson et al., 1982; J. L. Anderson, 1989; Prieve et al., 1984, 1984). Therefore, self-generated concentration gradient of near-by particles could affect an active colloid's migration apart from hydrodynamic interactions. This interaction, originating from the active colloid's chemical concentration profile distortion, is the so-called *phoretic* interaction and could be the dominant interaction between the active colloids depending on the particle's geometry and surface activity (Ibrahim & Liverpool, 2016; Soto & Golestanian, 2014; Uspal et al., 2015).

The behaviour of active particles not powered by a chemical concentration gradient (e.g., bacteria) are well predicted by the squirmer model (Berke et al., 2008; Spagnolie & Lauga, 2012). The squirmer model is a purely hydrodynamic model of an active particle experiencing no body force (i.e., zero net force). The model was first introduced by (Lighthill, 1952) and later used by (Blake, 1971) to describe the flow field generated by a beating cilia of paramecium. Even though the squirmer model was successful in describing the behaviour of non-chemically powered active particles, it's rather inadequate for describing the behaviour of chemically powered active colloids. The interactions between the latter are mediated by both hydrodynamic as well as chemical concentration gradients. Chemically powered active particles pair interactions as well as interaction with bounding surfaces are well understood (Ibrahim & Liverpool, 2015, 2016; Liebchen & Löwen, 2019; Liebchen & Mukhopadhyay, 2021; Uspal et al., 2015).

However, it's not clear from the literature how the presence of an externally imposed macroscopic chemical concentration gradient will affect the active colloids pair interactions. Therefore, we performed far-field analytical calculations, using method of images/reflections techniques, to obtain the effects of an external gradient on the active colloid's pair interactions.

Our main contribution in this work is that: (1.) we found an explicit expression for the interaction of the active colloids pair and (2.) we found a stable stationary configuration of the active colloids at a fixed separation and orientation relative to the direction of the imposed gradient.

In the next section, we introduce the problem setup and the mathematical model. We thereafter describe the method of reflections methodology. Finally, we present the results, discuss the results implications, and then conclude.

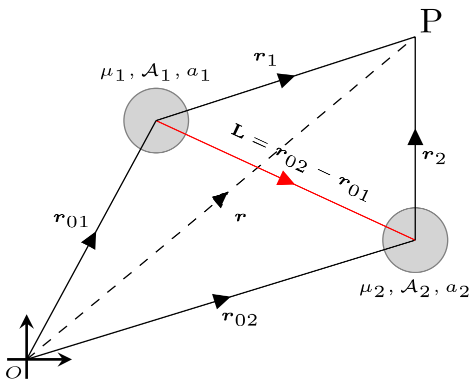

Figure 1: The active colloids sketch

THE MODEL

We consider spherical colloid particles with radius $\boldsymbol{a_1}$ and $\boldsymbol{a_2}$, *isotropic* chemical activity $\boldsymbol{A_1}$ and $\boldsymbol{A_2}$, mobility $\boldsymbol{\mu_1}$ and $\boldsymbol{\mu_2}$ suspended in an aqueous solution (see the pair setup sketch in Fig. 1). We also assume the solution viscosity is $\sim\mathbf{10^{-3}}\ \boldsymbol{Pa\cdot s}$ and density $\sim\mathbf{1}\boldsymbol{kg/m^3}$. Typical size of these colloids is $\sim\mathbf{1}\ \boldsymbol{\mu m}$ and move with a characteristic speed of $\sim\mathbf{1}\ \boldsymbol{\mu m/s}$. Thus, viscous forces dominate in this regime since the Reynolds number (Re) is negligible, Re $\sim\mathbf{10^{-3}} \ll \mathbf{1}$. Therefore, we model the colloid particles as mesoscopic particles immersed in a fluid with dissolved chemical molecules. Therefore, we write the continuum conservation equations for both mass (reaction-diffusion equations) and momentum (Stokes equations) (J. L. Anderson, 1989; Happel & Brenner, 1973; Kim & Karilla, 1991).

Mass conservation: The solute concentration field $\mathbf{c}(\mathbf{r})$ satisfy the Laplace equation

(1.) $$\nabla^2 c(r) = 0\ ,$$

where c(r) is the chemical concentration profile. The chemical activities A_1 particle 1 and A_2 for particle 2 engenders the boundary conditions

(2.)
$$-D\,\hat{n}_1\cdot\nabla c \quad = A_1 \quad \text{at} \quad r_1 = a_1\ ,$$
$$-D\,\hat{n}_2\cdot\nabla c \quad = A_2 \quad \text{at} \quad r_2 = a_2\ ,$$

on each particle. We note that throughout this article, we consider homogeneous surface chemical activities (i.e., A_1, A_2 are constants). We define the position vectors with origins at the particles centre: $\mathrm{r_1 = r - r_{01}}$ for particle 1 and $\mathrm{r_2 = r - r_{02}}$ for particle 2. Also, an imposed macroscopic gradient $\mathrm{A_\infty}$ along the direction $\hat{\mathrm{e}}_\mathrm{x}$ (see Fig. 1) gives rise to the far-field condition

(3.) $$\mathrm{c(r) \to c_\infty + (A_\infty/D)\,\hat{e}_x\cdot r \quad as \quad r\to\infty}\ .$$

Stokes's flow: The flow field $\mathbf{v}(\mathbf{r})$ satisfy the stokes equations (J. L. Anderson, 1989; Happel & Brenner, 1973)

(4.) $$\mathrm{\eta\,\nabla^2 v - \nabla p = 0\ , \qquad \nabla\cdot v = 0}\ ,$$

where p(r) is the pressure field and η is the dynamic viscosity of the fluid. At the surface of the particles, the flow field satisfy the boundary conditions

(5.)
$$\mathrm{v \quad = U_1 + a_1\hat{n}_1\times\Omega_1 + v_1^s\ , \quad at \quad r_1 = a_1}\ ,$$
$$\mathrm{v \quad = U_2 + a_2\hat{n}_1\times\Omega_2 + v_2^s\ , \quad at \quad r_2 = a_2}\ ,$$

where $\mathrm{a_1}$ is the radius of the particle 1, $\mathrm{U_1}$ and Ω_1 are the rigid body linear and angular velocities respectively. The slip velocities $\mathrm{v_{1,2}^s}$ are defined $\mathrm{v_{1,2}^s = \mu_{1,2}\left(\mathbb{1} - \hat{n}_{1,2}\otimes\hat{n}_{1,2}\right)\cdot\nabla c}$ with $\mu_{1,2}$ being the mobilities for particle 1 and particle 2 respectively. In addition, the fluid is quiescent far from the particles, i.e.

(6.) $$\mathrm{v\to 0\ , \quad as \quad r_1, r_2 \to \infty}\ .$$

The system of equations (1-6) is not closed because the rigid body velocities $\mathrm{U_{1,2}}$ and $\Omega_{1,2}$ are not known, and in fact they are the subject of the analysis. Therefore, to close the system of equations we note that the net force and torque on the particles vanishes (J. L. Anderson, 1989):

(7.)
$$\mathrm{F_k = \oiint \Pi\cdot\hat{n}_k\,dS_k = 0\ , \quad k = 1{,}2}\ ,$$
$$\mathrm{\Omega_k = \oiint a_1\hat{n}_1\times(\Pi\cdot\hat{n}_k)\,dS_k = 0\ , \quad k = 1{,}2}\ .$$

Note that $\oiint$ is a particle surface integral and Π is the Newtonian stress tensor for incompressible fluid defined as

(8.) $$\mathrm{\Pi = -p\mathbb{1} + \tfrac{\eta}{2}\left(\nabla\otimes v + (\nabla\otimes v)^T\right)}\ ,$$

where $\mathbb{1}$ is the 3 × 3 unit matrix and ⊗ is the tensor product.

THE METHOD OF REFLECTIONS

The goal of the analysis is to obtain equations of motion for the colloid particles. Dynamical behaviour of the particles could then be deduced by solving the resulting dynamical system. Therefore, the equations of motion are obtained from the approximate solution of the mass and momentum conservation equations using the method of reflections/images.

We briefly describe the method of images/reflections in this section. Interested reader may find the detailed derivation and discussion of the singularity solutions for the flow field in (Ibrahim & Liverpool, 2016; Spagnolie & Lauga, 2012). Also, extensive discussion on the image singularities for the chemical concentration field could be found in (Ibrahim & Liverpool, 2015, 2016), which are articles co-authored by one of the authors here.

It's noteworthy that both the mass conservation equation (1) and the stokes equations (4) for the momentum conservation are linear. We can therefore employ the method of reflections to obtain approximate solution to the equations (1) and (4). This method has its origin in solving electrodynamics problems, but now adopted for hydrodynamic problems (Andelman, 2004; Ibrahim & Liverpool, 2015).

Now, to simplify the presentation, we describe the procedure of obtaining the flow and chemical concentration fields from particle 1. However, similar procedure applies for particle 2. Therefore, since both the mass and momentum conservation equations are linear, let's then assume that the concentration and the flow fields can be written as the superposition of fields that each solves a simple sub-problem together with its associated boundary condition. i.e.

$$\begin{aligned} c(r) &= c^{(0)}(r) + c^{(1)}(r) + \cdots \\ v(r) &= v^{(0)}(r) + v^{(1)}(r) + \cdots , \end{aligned} \tag{9.}$$

where $c^{(0)}(r)$ consist of a sum of singularity solutions that satisfy independently the boundary conditions on the surface of the particles and the imposed concentration gradient (eqn. 3). equation for $c^{(0)}(r)$ is then solved for particle 1, together with the corresponding boundary condition on the particle 1 in isolation. Then, this chemical field emanating from particle 1 will not satisfy the boundary condition on particle 2. To correct for this, another singularity solution, $c^{(1)}(r)$, satisfying the Laplace equation is placed at the centre of particle 2. The procedure is repeated, swapping particle 1 with particle 2. We report the resulting solution of this procedure from both particles 1 and 2 in the next section.

RESULTS

In this section, we highlight the main results of our analysis. First, we present the approximate solutions for both the mass and momentum conservation equations and then subsequently present the resulting rigid body dynamical equations for the particles.

Concentration field: To obtain the concentration profile, we solve the coupled diffusion equations (1) subject to the boundary condition on both the particles surfaces (eqns. 2 and 5) and the far-field condition (eqn. 3). Using the method of images/reflections (briefly described above), we obtain the leading order chemical concentration field to be

$$c(r) = c_\infty + \frac{A_\infty}{D}\hat{e}_x \cdot r + \frac{A_1 a_1^2}{D\, r_1} + \frac{A_2 a_2^2}{D\, r_2} + \frac{a_1^3}{2D\, r_1^2} w_2 \cdot \hat{r}_1 - \frac{a_2^3}{2D\, r_2^2} w_1 \cdot \hat{r}_2 , \tag{10.}$$

where we define $w_1 = A_\infty\, \hat{e}_x - (A_1 a_1^2/L^2)\hat{L}$ and $w_2 = A_\infty\, \hat{e}_x + (A_2 a_2^2/L^2)\hat{L}$. A dimensionless plot of the chemical field above for $A_\infty/A_0 = 1$ can be found in Fig. 4.

Flow field: Similarly, the Stokes equations (4) are linear, and we can also iteratively solve an amenable set of simple problems; each solution satisfying a boundary condition on an active particle surface (see the brief description of the method of reflections above). Combining the leading order multipole solutions gives the fluid flow field due to the chemical concentration gradient

$$v(r) = \frac{1}{2}\left(3\frac{r_1 \otimes r_1}{r_1^5} - \frac{\mathbb{1}}{r_1^3}\right) \cdot U_1 + \frac{1}{2}\left(3\frac{r_2 \otimes r_2}{r_2^5} - \frac{\mathbb{1}}{r_2^3}\right) \cdot U_2 \tag{11.}$$

where we note that $\otimes$ is the tensor product. A two-dimensional slice of the streamlines of this flow field for $A_\infty/A_0 = 1$ has been plotted in Fig. 2 (masking particle 2) and Fig. 3 (for both the particles).

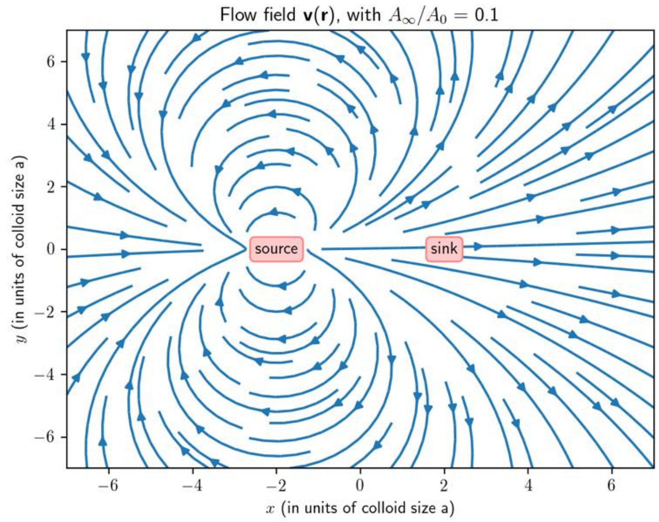

Figure 2: Active colloid (single) particle flow field

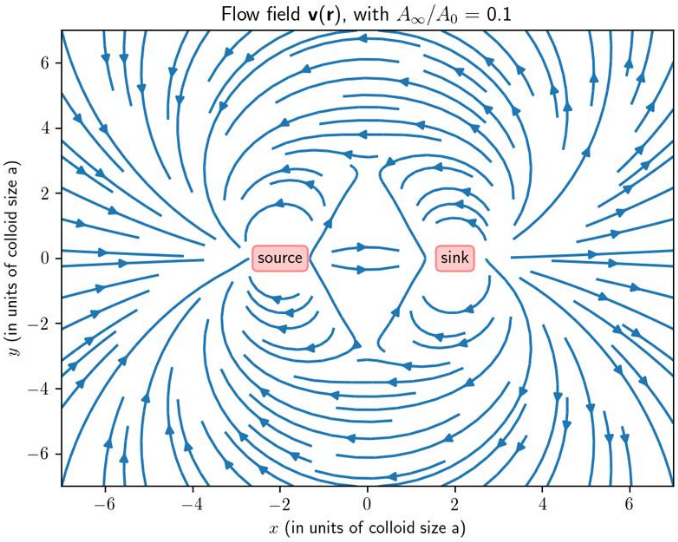

Figure 3: Active colloids dipole flow field, v(r)

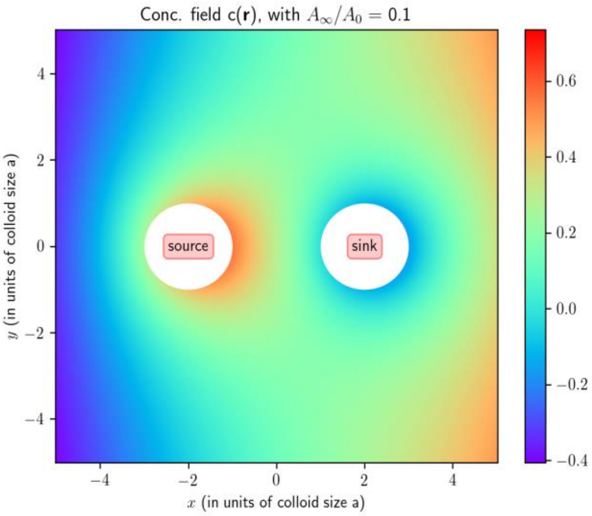

Figure 4: Active colloid dipole concentration field, c(r)

Rigid body motion

Substituting the chemical concentration field (eqn. 10) and the flow field (eqn. 11) into the force and torque balance equations (eqn. 7), we obtain the rigid body motion $(\boldsymbol{U_1}, \boldsymbol{\Omega_1}, \boldsymbol{U_2}, \boldsymbol{\Omega_2})$ of the active colloids. In the laboratory frame of reference, the origin O in the sketch (Fig. 1) is stationary and the rigid body velocities for the two active colloid particles are

$$\begin{aligned} \mathrm{U}_1 &= -\frac{\mu_1}{3D}\left(A_\infty\,\hat{\mathbf{e}}_x + \frac{A_2 a_2^2}{L^2}\hat{\mathbf{L}}\right) , \\ \mathrm{U}_2 &= -\frac{\mu_2}{3D}\left(A_\infty\,\hat{\mathbf{e}}_x - \frac{A_1 a_1^2}{L^2}\hat{\mathbf{L}}\right) . \end{aligned} \tag{12.}$$

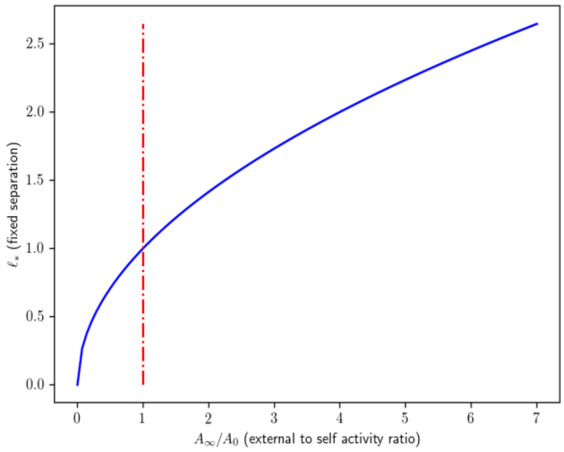

Figure 5: Active colloids pair separation with external field strength.

Here, due to the active colloid's symmetry, chemical activity homogeneity (constant $\boldsymbol{A}$) and mobility isotropy (constant $\boldsymbol{\mu}$) of the particles, the angular velocities vanish, i.e., $\boldsymbol{\Omega_1} = \mathbf{0}$, $\boldsymbol{\Omega_2} = \mathbf{0}$. Note that, neglecting Brownian motion, a chemically isotropic active colloid is stationary (immobile) if it's isolated from any other particle and no external chemical gradient. That is, these particles, unlike half-coated Janus particles with chemical anisotropy on their surfaces, do no self-propel, but rather becomes mobile only in response to chemical gradients generated by other particles and/or external potential gradients.

Pair centre of mass and relative position evolution

We define the displacement between the two active colloids as $\mathbf{L}$ (see the sketch in Fig. 1). Therefore, the pair separation $\mathbf{L} = \mathbf{r}_{02} - \mathbf{r}_{01}$ and the center of mass $\mathrm{R}_{\mathrm{cm}} = \mathbf{r}_{02} + \mathbf{r}_{01}$ evolves according to the equations

(13.) $\frac{d}{dt}\mathbf{L} = \mathrm{U}_2 - \mathrm{U}_1$ and $\frac{d}{dt}\mathrm{R}_{\mathrm{cm}} = \mathrm{U}_2 + \mathrm{U}_1$.

From the above equations (12 and 13) we obtain the main contribution of this paper:

(14.)
$$\frac{d}{dt}\mathrm{L} = \frac{(\mu_1 - \mu_2)}{3D} A_\infty\, \hat{\mathbf{e}}_x + \frac{(\mu_1 A_2 a_2^2 + \mu_2 A_1 a_1^2)}{3DL^2}\hat{\mathrm{L}} .$$

This equation gives an inter-particle interaction between the colloid particles that could then be used in molecular dynamics simulations. Therefore, the main parameters controlling this pair interaction are the active colloid's surface chemical activity $A_{1,2}$, mobilities $\mu_{1,2}$ and sizes $a_{1,2}$. Note the quadratic dependence of the interaction with the pair sizes. This is reminiscent of the high surface-to-volume ratio of these active colloids with microscopic dimensions.

Henceforth, we consider particles with their chemical activities $A_1 = A_2 = A_0$ (a constant), radius $a_1 = a_2 = a$ (a constant) and their mobilities $|\mu_1| = |\mu_2| = \mu_0 > 0$ (a constant). Now, we have a natural length scale in the system, the particle radius a. Then, the dimensionless inter-particle separation is $\boldsymbol{\ell} = \mathbf{L}/a$ while the dimensionless speed is $U^* = (\mu_0 A_0/3D)$ such that $\mathcal{U}_1 = \mathbf{U}_1/U^*$, $\mathcal{U}_2 = \mathbf{U}_2/U^*$ and the dimensionless time $\tau = a/U^*$. Therefore, the evolution of the pair of particles separation $\boldsymbol{\ell}$ can be computed from the dynamical equations

(15.)
$$\begin{aligned} \frac{d\ell}{d\tau} &= \hat{\boldsymbol{\ell}} \cdot (\mathcal{U}_2 - \mathcal{U}_1) , \\ \frac{d\hat{\boldsymbol{\ell}}}{d\tau} &= \left(\mathbb{1} - \hat{\boldsymbol{\ell}}\,\hat{\boldsymbol{\ell}}\right) \cdot (\mathcal{U}_2 - \mathcal{U}_1) . \end{aligned}$$

In the same vein, we define the pair centre of mass as $\mathcal{R}_{\mathrm{cm}} = \mathbf{r}_{01} + \mathbf{r}_{02}$ and therefore evolves according to the dynamical equations

(16.) $\frac{d}{d\tau}\mathcal{R}_{\mathrm{cm}} = \mathcal{U}_1 + \mathcal{U}_2$.

Therefore, we can write the dimensionless equations for the inter-particle separation, $\boldsymbol{\ell}$, the pair center of mass, $\mathcal{R}_{\mathrm{cm}}$ and the relative rotation of the two particles as follows:

(17.) $\frac{d}{d\tau}\mathcal{R}_{\mathrm{cm}} = \mathbf{0}$,

for the centre of mass. This implies that two particles will Defining $\hat{\boldsymbol{\ell}} = (\cos\theta, \sin\theta, 0)$,

(18.)
$$\begin{aligned} \frac{d\ell}{d\tau} &= 2\tilde{A}_\infty\, \hat{\mathbf{e}}_x \cdot \hat{\boldsymbol{\ell}} - \frac{2}{\ell^2} , \\ \frac{d\theta}{d\tau} &= -2\frac{\tilde{A}_\infty}{\ell}\sin\theta . \end{aligned}$$

where $\tilde{A}_\infty = A_\infty/A_0$. Note that we ignore the Brownian random fluctuation contribution in the equation above. This is to allow us to study, in isolation, the competing effects of the external chemical gradient and the phoretic interaction effects. In the steady state, the time derivatives vanish, and the particles relative position and orientation are fixed and given by

(19.)
$$(\ell_*, \theta_*) = \begin{cases} \left(\sqrt{\tilde{A}_\infty}\,,\, 0\right) , & \text{if } \tilde{A}_\infty > 0 \\ \left(\sqrt{-\tilde{A}_\infty}\,,\, \pi\right) , & \text{if } \tilde{A}_\infty < 0 \end{cases} .$$

This implies the pair will form a *dipole* with a fixed separation ℓ^*. Linear stability analysis shows that this fixed point is stable.

DISCUSSION

We have calculated the interaction of chemically isotropic active colloid particles in an external chemical concentration gradient. Further analysis of the resulting dynamical system (eqn. 18) shows that a stable configuration of the pair of active colloids is formed for a chosen combination of the particles physico-chemical parameters. To isolate the effects of the chemical gradient and the hydrodynamic flow fields, we neglect the background Brownian motion of the particles in the dynamical equations (18).

This interesting result comes from the balance of different competing effects. First, we have the hydrodynamic interaction that, to the leading order, decays as $1/r^3$ source-dipole singularity field (see eqn. 11) (Ibrahim & Liverpool, 2016; Spagnolie & Lauga, 2012). Secondly, the phoretic interaction between the pair of particles decays much slowly as $1/r^2$ via the surface slip velocity on each of the particles (see eqn. 5). The last contribution comes from the $O(1)$ external chemical gradient induced migration of the active colloids (see eqn. 12).

These competing effects leads to the formation of the stable dipole configuration of the pair of active colloids (eqn. 19). It is important to note that this behaviour is beyond the scope of the simple hydrodynamic squirmer model since the phoretic interaction is a distinct physical mechanism. This highlights, once again, the importance of accounting for the phoretic interaction for these active systems. Another noteworthy observation is the fact that in the absence of the externally imposed chemical gradient, the active colloids will either coalesce or disperse depending on the physico-chemical of the particles (Buttinoni et al., 2013; Soto & Golestanian, 2014).

(Soto & Golestanian, 2014) performed extensive molecular dynamics simulations for a large collection of similar active colloids to the model system we study in this article without the external chemical gradient. The authors predicted, depending on the properties of the active colloids, the formation of self-assembling colloidal 'molecules' that dynamically merge, break, rotate and sometimes shows persistent linear motion in addition to the Brownian random motion. Thus, this articles' prediction of active colloids *dipole* formation could expand the range of possible emergent structures that may arise from a large of such particles. The multitude of emergent dynamic structures arising the competition between the hydrodynamic and phoretic effects points to the potential role that chemically powered active colloids might play in the future design of smart materials.

The calculated inter-particle interaction between the two active colloids with respective mobility $\mu_{1,2}$, chemical activity $A_{1,2}$ and radii $a_{1,2}$ (see Figure 1) could be employed in a molecular dynamics simulation for understanding the collective behaviour of novel active colloids suspension. Carefully chosen physico-chemical properties of the active colloids, we predict a formation of a stable dipole of pair of active colloids having fixed separation and orientation relative to an external chemical gradient (see eqn. 19 and Fig. 5). This could provide an additional chemical control mechanism for artificially synthesised active matter systems.

CONCLUSION

We have studied the interactions of chemically active colloid particles in the presence of an externally imposed gradient. We obtained explicit inter-particle interactions for the active colloids. Choosing a combination of the colloids' physico-chemical properties, we found that a pair of chemically active colloids could form a stable dipole with a separation that can be controlled with the strength of the external chemical gradient. This, perhaps, could be a plausible route to control a self-assembling smart material composed of chemically active colloids. In addition, these results could help in understanding emergent phenomena of the active colloid systems. In future work, it will be interesting to investigate the complex behaviour of a large collection of such active colloids in the presence of the external chemical gradient via molecular dynamics simulation.

REFERENCES

Andelman, D. (2004). *Introduction to Electrostatics in Soft and Biological Matter*.

Anderson, J. L. (1989). Colloid transport by interfacial forces. *Annual Reviews of Fluid Mechanics*, *21*, 61–99.

Anderson, J., Lowell, M., & Prieve, D. (1982). Motion of a particle generated by chemical gradients Part 1. Non-electrolytes. *Journal of Fluid Mechanics*, *117*, 107–121.

Berke, A. P., Turner, L., Berg, H. C., & Lauga, E. (2008). Hydrodynamic attraction of swimming microorganisms by surfaces. *Physical Review Letters*, *101*(3), 038102.

Bialké, J., Speck, T., & Löwen, H. (2015). Active colloidal suspensions: Clustering and phase behavior. *Journal of Non-Crystalline Solids*, *407*, 367–375. https://doi.org/10.1016/j.jnoncrysol.2014.08.011

Blake, J. (1971). A spherical envelope approach to ciliary propulsion. *Journal of Fluid Mechanics*, *46*(01), 199–208.

Buttinoni, I., Bialké, J., Kümmel, F., Löwen, H., Bechinger, C., & Speck, T. (2013). Dynamical clustering and phase separation in suspensions of self-propelled colloidal particles. *Physical Review Letters*, *110*(23), 238301.

Cates, M. E., & Tailleur, J. (2015). Motility-Induced Phase Separation. *Annual Review of Condensed Matter Physics*, *6*(1), 219–244. https://doi.org/10.1146/annurev-conmatphys-031214-014710

Ebbens, S., Gregory, D. A., Dunderdale, G., Howse, J. R., Ibrahim, Y., Liverpool, T. B., & Golestanian, R. (2014). Electrokinetic effects in catalytic platinum-insulator Janus swimmers. *EPL (Europhysics Letters)*, *106*(5), 58003.

Ebbens, S. J., & Howse, J. R. (2010). In pursuit of propulsion at the nanoscale. *Soft Matter*, *6*(4), 726–738.

Eze, I. I., & Joseph, E. (2018). Phase behavior of hard-sphere particle in a Colloidal binary mixture. *FUDMA JOURNAL OF SCIENCES-ISSN: 2616-1370*, *2*(1), 43–47.

Golestanian, R., Liverpool, T., & Ajdari, A. (2007). Designing phoretic micro-and nano-swimmers. *New Journal of Physics*, *9*(5), 126.

Happel, J., & Brenner, H. (1973). *Low Reynolds number hydrodynamics* (Second). Noordhoff international publishing.

Howse, J. R., Jones, R. A., Ryan, A. J., Gough, T., Vafabakhsh, R., & Golestanian, R. (2007). Self-motile colloidal particles: From directed propulsion to random walk. *Physical Review Letters*, *99*(4), 048102.

Ibrahim, Y., & Liverpool, T. B. (2015). The dynamics of a self-phoretic Janus swimmer near a wall. *EPL (Europhysics Letters)*, *111*(4), 48008.

Ibrahim, Y., & Liverpool, T. B. (2016). How walls affect the dynamics of self-phoretic microswimmers. *The European Physical Journal Special Topics*, *225*(8), 1843–1874.

Jewell, E. L., Wang, W., & Mallouk, T. E. (2016). Catalytically driven assembly of trisegmented metallic nanorods and polystyrene tracer particles. *Soft Matter*, *12*(9), 2501–2504.

Kim, S., & KARILLA, S. (1991). *Microhydrodynamics*. Butterworth-Heinemann Publish.

Kreuter, C., Siems, U., Nielaba, P., Leiderer, P., & Erbe, A. (2013). Transport phenomena and dynamics of externally and self-propelled colloids in confined geometry. *The European Physical Journal Special Topics*, *222*(11), 2923–2939.

Liebchen, B., & Löwen, H. (2019). Which interactions dominate in active colloids? *The Journal of Chemical Physics*, *150*(6), 061102 %@ 0021-9606.

Liebchen, B., & Mukhopadhyay, A. K. (2021). Interactions in active colloids. *Journal of Physics: Condensed Matter*, *34*(8), 083002.

Lighthill, M. (1952). On the squirming motion of nearly spherical deformable bodies through liquids at very small Reynolds numbers. *Communications on Pure and Applied Mathematics*, *5*(2), 109–118.

Moran, J. L., & Posner, J. D. (2017). Phoretic Self-Propulsion. *Annual Review of Fluid Mechanics*, *49*, 511–540.

Navarro, R. M., & Fielding, S. M. (2015). Clustering and phase behaviour of attractive active particles with hydrodynamics. *Soft Matter*, *11*(38), 7525–7546.

Negro, G., Caporusso, C. B., Digregorio, P., Gonnella, G., Lamura, A., & Suma, A. (2022). *Inertial and hydrodynamic effects on the liquid-hexatic transition of active colloids* (arXiv:2201.10019). arXiv. https://doi.org/10.48550/arXiv.2201.10019

Palacci, J., Sacanna, S., Steinberg, A. P., Pine, D. J., & Chaikin, P. M. (2013). Living crystals of light-activated colloidal surfers. *Science*, *339*(6122), 936–940.

Paxton, W. F., Sen, A., & Mallouk, T. E. (2005). Motility of catalytic nanoparticles through self-generated forces. *Chemistry–A European Journal*, *11*(22), 6462–6470.

Prieve, D., Anderson, J., Ebel, J., & Lowell, M. (1984). Motion of a particle generated by chemical gradients. Part 2. Electrolytes. *Journal of Fluid Mechanics*, *148*, 247–269.

Soto, R., & Golestanian, R. (2014). Self-assembly of catalytically active colloidal molecules: Tailoring activity through surface chemistry. *Physical Review Letters*, *112*, 068301.

Spagnolie, S. E., & Lauga, E. (2012). Hydrodynamics of self-propulsion near a boundary: Predictions and accuracy of far-field approximations. *Journal of Fluid Mechanics*, *700*, 105–147.

Theurkauff, I., Cottin-Bizonne, C., Palacci, J., Ybert, C., & Bocquet, L. (2012). Dynamic clustering in active colloidal suspensions with chemical signaling. *Physical Review Letters*, *108*(26), 268303.

Uspal, W., Popescu, M. N., Dietrich, S., & Tasinkevych, M. (2015). Self-propulsion of a catalytically active particle near a planar wall: From reflection to sliding and hovering. *Soft Matter*, *11*(3), 434–438.

Wagner, M., Roca-Bonet, S., & Ripoll, M. (2021). Collective behavior of thermophoretic dimeric active colloids in three-dimensional bulk. *The European Physical Journal E*, *44*(3), 1–11.